Laboratory #3: Formula One

Logan B. Freeman[1]
MAE 4400 – Thermo-fluids labs, Logan, UT, 84322, USA

Abstract

This experiment investigates the effect of front wing height on Formula 1 car performance through wind tunnel testing and mathematical modeling. The study examines the aerodynamic properties and resulting lap times across six wing heights ranging from 1.2mm to 100.2mm. Measurements of lift and drag forces at various air velocities enabled calculation of non-dimensional coefficients and performance metrics under ground effect conditions. The wind tunnel data revealed optimal performance at 19.6mm height, where maximum ground effect produced the fastest lap time of 70.10 ± 0.08 seconds, approximately 2.5 seconds faster than a wingless configuration. At extremely low heights (1.2mm), a flutter phenomenon resembling "porpoising" created unstable conditions and reduced performance. As wing height increased beyond the optimal position, both lift and drag coefficients gradually decreased and plateaued, indicating diminished ground effect influence. The results quantified the fundamental performance trade-off between straight-line speed and cornering capability, with the optimal configuration balancing these competing factors. Experimental limitations included wind tunnel flow fluctuations and simplified lap time modeling assumptions. The study demonstrates the critical importance of wing height optimization in competitive motorsport applications while providing quantitative data on ground effect aerodynamics. Suggested improvements include more sophisticated flow uniformity control and development of a more comprehensive lap time model incorporating transient vehicle dynamics.

Nomenclature

A = area
a = coefficient for tire force
b = coefficient for tire force
C_D=drag coefficient
C_L=lift coefficient
g = gravitational acceleration (9.8m/s^2)
P = power
m = mass
r = turn radius
Re = Reynolds number
ρ = air density
t = time
V = velocity
σ = uncertainty

Subscripts

c = cornering

s = straight-line

I. Introduction

FORMULA One racing (F1) is the most popular open-wheel racing discipline on the planet. Teams spend upwards of $100 million yearly to perfect their car. Incremental improvements and fine-tuned adjustments are desired, as top

[1] Senior, Mechanical & Aerospace Engineering, A02302894

cars have lap times separated from each other by mere hundredths of a second. The aerodynamic package of an F1 car is an important part of its performance. The aerodynamic package consists mainly of a front wing and a rear wing. The wings exist to provide downforce for a minimum amount of drag. Downforce allows F1 cars to sustain higher cornering speeds, and lower drag allows for higher straight line speeds.

F1 teams spend millions specifically on aerodynamic analysis. Two methods for aerodynamic analysis are Computational Fluid Dynamics (CFD) and Wind Tunnel analysis. CFD entails modeling a car, or a car part, in a Computer-Aided Design (CAD) software, and then numerically solving the flow around the car or car part. CFD has improved greatly in the last 30 years and can now accurately and quickly predict the aerodynamics around a vehicle. However, the best tests are still wind tunnel tests, because wind tunnels naturally feature coupled physics between the structure and aerodynamics. As a demonstration of the value of wind tunnel testing in F1, total wind tunnel test hours are limited by the International Automobile Federation (FIA) for the winning teams as a handicap.

One important consideration is the front wing height. As a rule of thumb, when a wing is within a distance less than the wingspan from the ground, increased lift is observed without an increased drag cost. This is due to interaction of wingtip vortices with the ground. Ground effect is generally stronger closer to the ground. However, at close distances to the ground, aerodynamic flutter is observed. In F1 cars, the flutter manifests itself as “porpoising”.

This detrimental effect is caused when the low pressure under the car pulls the car to the ground. This causes the flow to stall, creating increased drag and allowing the car to rise. When the car rises, the flow can reattach and pull the car down again. This effect is detrimental to both the suspension and the driver. In the 2022 season porpoising was particularly bad and the FIA developed new regulations to control porpoising for driver safety.

In this experiment, the authors are interested in optimizing the airfoil height for a race car to complete a lap of a 1 mile oval, with two 400m straights bracketed by two 400m curves.

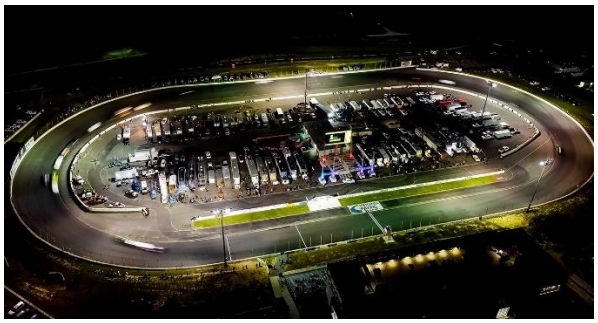

Figure 1: Overhead view of oval racetrack [1].

To achieve the highest straight-line speed, minimum drag is desired. To achieve the highest cornering speed, maximum downforce is desired. Producing increased downforce comes at the cost of increased drag. Therefore, the fastest lap time is a trade-off between speed on the curves and straights. In this analysis of a lap time, the acceleration and deceleration period between the curves and straights is assumed to be negligible.

In this experiment, an airfoil will be positioned at different heights above the ground, and at different flow velocities. Lift and drag on the airfoil will be measured. Based on the measured lift and drag, a lap time will be calculated, and the optimal configuration for the fastest lap will be calculated.

A simple uncertainty analysis is performed. Sources of uncertainty and error are identified and quantified. Conclusions are drawn about the performance of the airfoil and resulting F1 car, and suggestions are made for improvements on accuracy in future experiments.

II. Methods

The methodology and experimental setup for measuring the lift and drag on the airfoil are described. In addition, the equations used to evaluate the lift and drag and predict the lap time are also calculated.

A. Wind Tunnel & Load Cells

The wind tunnel available is a closed-circuit tunnel with a large test section. The wind tunnel is designed to produce uniform flow up to a minimum of 35m/s. A fan drives the flow in the tunnel, and a computer control unit through LabView modulates the fan to achieve the desired fan speed. A grid is present in the tunnel to produce homogenous, isotropic turbulent conditions in the flow. A depiction of a closed-circuit wind-tunnel is included below.

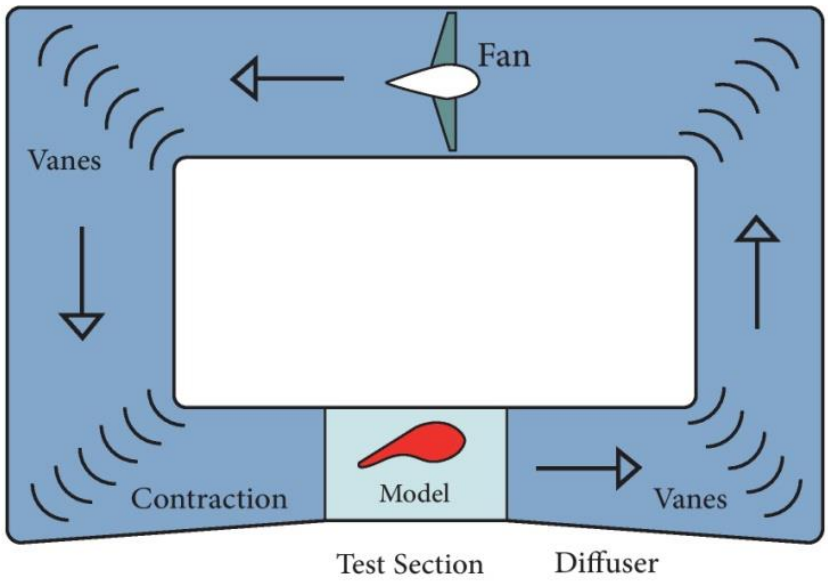

Figure 2: Generalized Depiction of Closed-Circuit Wind Tunnel [2].

The test section has exceptional optical accessibility. However, no optical instrumentation was used in this experiment. Instead, two load cells were installed in the test section, one to measure lift and the other to measure drag. The load cells are directed through LabView, which outputs their voltage readings directly. The load cell has an uncertainty of +/- 0.02V.

A calibration is performed on the load cell with known weights. The results of the calibration and associated uncertainty are available in the Results section. A linear fit is used for both the drag and lift load cells.

B. Experimental Procedure & Data Collection

Six tests of height are to be conducted in the experiment, spanning from the ground to 100mm. In addition, six velocities will be tested, spanning 5m/s to 30m/s. This results in a matrix of 36 individual test points to be collected.

In each configuration, the airfoil is mounted at the desired height. The height is measured using digital calipers which have an uncertainty of 0.01mm. Then, the wind tunnel test section is sealed and the wind tunnel is started. Each of the six velocities is stepped through in the wind tunnel, waiting for the speed in the tunnel to stabilize before collecting data. Data is collected for approximately 10 seconds for each data point at a rate of 20Hz. For processing purposes, the test section velocity and load cell readings are averaged during the 10s period.

A depiction of the wing is below. The apparatus for changing the height is clearly visible. The wing dimensions were measured as a chord of 115mm and a span of 582mm. Therefore, the wing area is $0.06693 m^2$. The uncertainty in these measurements is 0.01mm based on the digital calipers the wing was measured with. The resultant uncertainty in the area is $6.97*10^{-6}$, which corresponds with a 0.0104% uncertainty. Because this uncertainty is so low compared to voltage and velocity uncertainties, the uncertainty of the wing area will be neglected in the calculation of uncertainties through the rest of the lab.

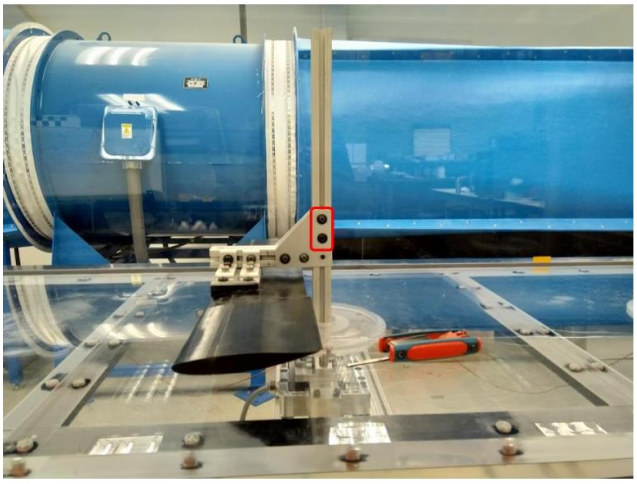

Figure 3: Wing Mounted in Wind Tunnel. The Span is into the Page, and the Chord is from Left to Right [3].

C. Lift & Drag

The lift and drag are measured using the load cells. These are non-dimensionalized using the dynamic pressure into a lift and drag coefficient:

$$C_L = 2\frac{F_L}{A\rho V^2}$$

$$C_D = 2\frac{F_D}{A\rho V^2}$$

The dynamic pressure is calculated based on the density and tunnel velocity. The density is assumed to be equal to atmospheric density at the altitude of Utah State University, or 1.0 kg/m^3. The assumption of constant density or incompressibility is valid, since the flow stays below Mach 0.3. The velocity is measured by the tunnel and has an uncertainty of +/- 0.1m/s. The wetted area in consideration is the wing area, equal to the chord times the span.

D. Straight-line Speed

The straight-line speed of the car is driven by the drag. At steady conditions, the engine power is equal to the drag multiplied by the velocity:

$$P = F\,V$$

The drag is given by a combination of the drag from the car and drag from the wing:

$$F_D = \frac{1}{2}\rho V_s^2 (C_{D,car}A_{car} + C_{D,wing}A_{wing})$$

The drag coefficient and area of the car are 1 and 3m^2, respectively. The power is fixed at 100hp. Therefore, the velocity on the straight can be calculated as:

$$V_s = \sqrt[3]{\frac{2P}{\rho(C_{D,car}A_{car} + C_{D,wing}A_{wing})}}$$

The uncertainty of this quantity will be calculated in section IV.

E. Cornering Speed

When the car is in a corner, the speed is limited by the maximum cornering force, or the side force. In a turn, the centripetal acceleration tends to push the car outwards, away from the racing line of the curve. Cornering force is produced by the tires of the car. The cornering force is considered in this experiment to be a linear function of the downforce:

$$F_{cornering} = a\left(-F_{downforce}\right) + b$$

The coefficients a and b have values of $a = 0.198\frac{\mathrm{N}}{\mathrm{N}}$ and $b = 1\mathrm{N}$, respectively. To allow for the uncertainties to be calculated, the values Although the downforce to cornering force linear relation was given for one tire, the downforce is distributed evenly over all four tires, and so the relation holds for the total downforce.

In a maximum-performance turn, the cornering force is equal to the centripetal force:

$$\frac{mV_c^2}{r} = F_{cornering}$$

The cornering force is replaced by the linear fit:

$$\frac{mV_c^2}{r} = a\left(-F_{downforce}\right) + b$$

And the downforce is then substituted with the expression which includes the wing downforce, car downforce, and weight of the car:

$$\frac{mV_c^2}{r} = a\left(-\frac{1}{2}\rho V_c^2\left(C_{L,car}A_{car} + C_{L,wing}A_{wing}\right) + mg\right) + b$$

The lift coefficients are negative, so the total downforce is positive. The maximum cornering velocity can be isolated and solved for:

$$V_c = \sqrt{\frac{(a\,mg + b)}{\frac{m}{r} + \left(\frac{a}{2}\right)\rho\left(C_{L,car}A_{car} + C_{L,wing}A_{wing}\right)}}$$

The uncertainty of the maximum cornering velocity will be calculated and expressed in section IV.

F. Lap Times

As mentioned in the Introduction, the desired lap is one mile long and consists of two 400m straights and two 400m corners. The corners are 400m in length, so the turn radius is $r = \frac{400\mathrm{m}}{\pi} = 127.32m$. The lap time is then given by:

$$t_{lap} = 800\mathrm{m}\left(\frac{1}{\mathrm{V_s}} + \frac{1}{V_c}\right)$$

The uncertainty of the lap time depends on the uncertainty of the cornering and straight velocity, and will be calculated in section IV.

G. Limitations & Assumptions

There are several limiting assumptions in this experiment. First, the wind tunnel is assumed to produce uniform conditions. However, the time-history data clearly shows large mean flow velocity fluctuations in the tunnel. These fluctuations are time-averaged, however the nonlinear nature of fluid flow means that time-averaging the impacts of fluctuations reduces the accuracy of the experiment. In addition, the ground condition and confined flow affect the ground effect. Protuberances on the ground, and walls close to the wingtips both contribute to changing the ground effect, limiting the accuracy of the measurement of the lift and drag.

In the model, there are a few key assumptions. First, the assumption that the speed instantly changes between cornering and straight-line is a poor assumption. In fact, in F1, IndyCar, and other open-wheel racing disciplines, braking and accelerating is a very important factor in driver performance. Second, the assumption of a linear relationship between downforce and cornering force is limiting. In general, the amount of cornering force is not constant between tires. On an oval racing circuit, for example, the inner tire will generate much more cornering force than the outer tire. Tire temperature, compound, and wear also contribute to the cornering capacity of a tire.

Although there are both experimental limitations and model assumptions, this model and procedure are generally appropriate to analyze the performance of a wing on an F1 car.

III. Results

Initially, the lift and drag load cells must be calibrated. This calibration is performed as described in the Methods section. The calibration graph and equations of fit are provided below:

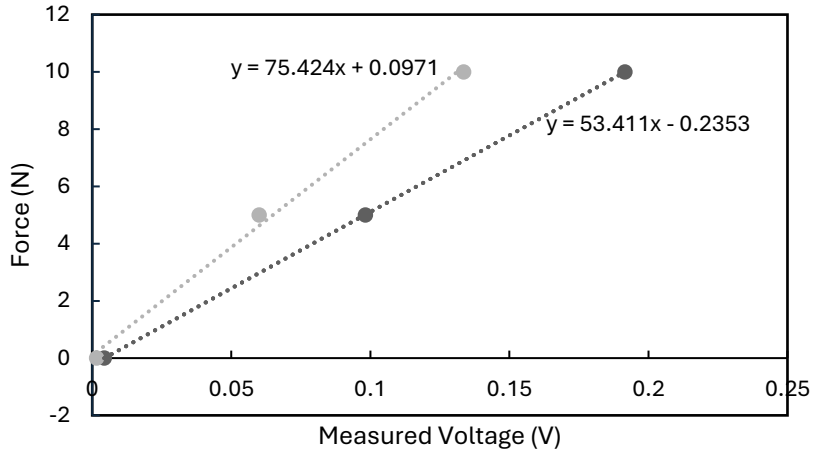

Figure 4: Calibration Curves for Lift and Drag.

The drag is in light gray, and the lift is in dark gray. Using the linear calibrations derived above, the lift and drag force can be calculated for each of the 36 test points. The lift and drag forces are presented in raw format below:

Table 1: Raw Lift Force (N) Across all Test Points

Velocity Set Point (m/s)	Airfoil height (mm)					
	1.2	19.6	40.4	60.0	80.2	100.2
5	-0.09	0.45	0.31	0.22	0.21	0.22
10	-0.26	2.22	1.8	1.31	1.1	1.02
15	-0.24	5.07	4.05	2.95	2.7	2.33
20	0.8	8.86	6.91	5.74	4.78	4.29
25	1.24	14.03	11.06	9.00	8.15	7.56

Table 2: Raw Drag Force (N) Across all Test Points

Velocity Set Point (m/s)	Airfoil height (mm)					
	1.2	19.6	40.4	60.0	80.2	100.2

5	0.62	0.39	0.44	0.36	0.21	0.33
10	1.71	1.57	1.59	1.63	1.56	1.51
15	3.77	3.33	3.4	3.48	3.44	3.6
20	7.35	5.71	6.1	6.08	5.97	6.15
25	9.97	8.87	9.37	9.47	9.68	9.21

In Table 1, the raw lift force appears to be negative at the lowest height. In the coordinate frame used in this experiment, that corresponds with an upwards lift. In a steady flow, this is clearly impossible for an airfoil angled downwards. However, a severe flutter mode was observed at the lowest mounting height. This flutter mode corresponds exactly with the porpoising observed in F1. Low-pressure areas are generated under the wing, which sucks the wing closer to the ground. This causes the air under the wing to slow down, which then causes the wing to rise. This flutter mode was severe enough to cause extremely chaotic data, and even a resultant average upwards lift. The flutter mode was not observed at the other heights.

The forces are nondimensionalized into coefficients as described in the Methods. They are plotted against the height non-dimensionalized by the chord. The figures for lift and drag are presented below:

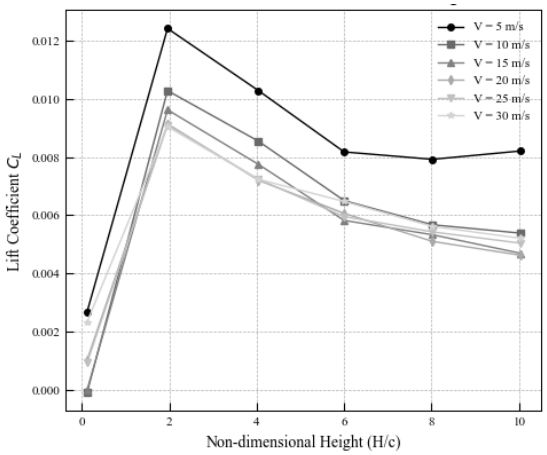

Figure 5: Lift Coefficient as a Function of Wing Height Non-dimensionalized by Chord.

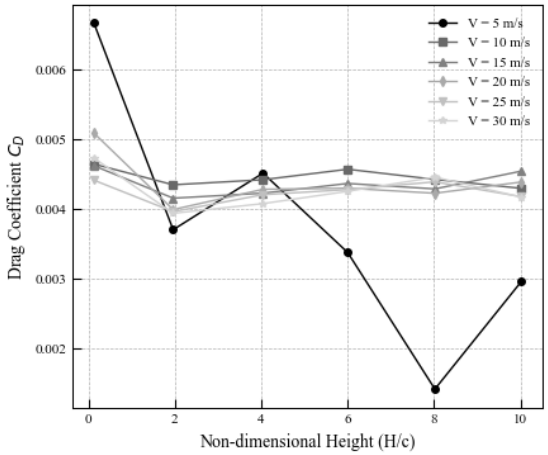

Figure 6: Drag Coefficient as a Function of Wing Height Non-dimensionalized by Chord.

In the above figure, the lift coefficients exhibit similar dependence on height. The lift is low at the lowest height, due to the flutter effect described earlier. The lift spikes because of ground effect, and then as the wing gets higher, the

magnitude of ground effect diminishes. The lift appears to be plateauing, which corresponds with the wing moving entirely out of ground effect. For the drag, the curves above 5 m/s exhibit near-identical behavior. Either the data at 5 m/s is too noisy, or an entirely different mechanism is responsible for drag production (for example, turbulence has not been tripped).

To analyze the effect of Reynolds number on lift and drag, a figure was generated to show the lift and drag dependence on Reynolds number:

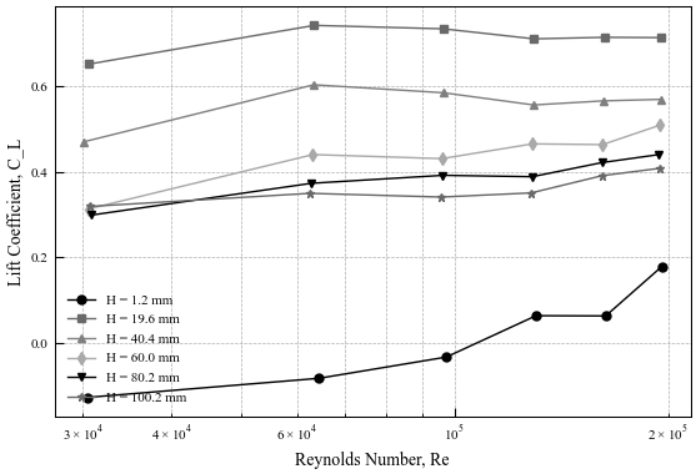

Figure 7: Lift Coefficient vs Reynolds Number (log-scaled)

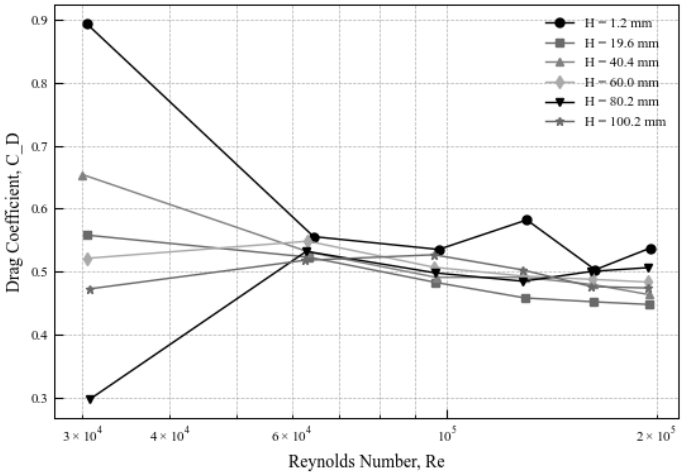

Figure 8: Drag Coefficient vs Reynolds Number (log-scaled)

To decide which data should be used, some analysis is necessary. First, the Reynolds number in flows the real car encounters are orders of magnitude higher, on the order of Re=1e6-1e7. The most important flow distinction between low and high Reynolds numbers is turbulence. At high Reynolds numbers, turbulence appears earlier and dominates drag production. Therefore, to best mimic the performance of the true race car, the lift and drag data from the highest Reynolds numbers will be used.

The Reynolds number is not the only characteristic which affects turbulent behavior. Another important characteristic is freestream turbulence. For example, an F1 car driving directly behind another car experiences higher drag and higher tire degradation, because the air it drives into is already turbulent. The wind tunnel mimics this effect. A screen in the wind tunnel generates a uniform, turbulent freestream flow, with a velocity fluctuation magnitude

much higher than the values of 1-2% observed in quiescent air. In this respect, the wind tunnel models turbulent effects well.

A short discussion on Mach number is also appropriate. In fluid flow, compressibility effects scale with the square of Mach number. In the wind tunnel, the maximum velocity was 35m/s, corresponding to a Mach number of approximately 0.1. In a real car, the number could be as high as 0.25. However, because of the square-scaling of compressibility, Mach effects are negligible and can safely be ignored in this regime.

Next, the total drag force, maximum straight-line speed, cornering force, and maximum cornering force are calculated. The wing lift and drag coefficients from the highest Reynolds-number tests are used. The results are displayed in the table below. The uncertainties for the lift coefficients are calculated as an intermediary step and displayed in the Appendix. The uncertainties of the forces and velocities are calculated and displayed alongside the values, following the methodology described in section IV.

Table 3: Calculated Drag Force, Cornering Force, Straight Speed, and Cornering Speed

Wing height (mm)	Total Drag Force (N)	Maximum Straight Speed (m/s)	Total Cornering Force (N)	Maximum Cornering Speed (m/s)
1.2	11218.0531 ± 107.4508	35.5352 ± 0.1135	432.8158 ± 0.6820	16.5782 ± 0.0131
19.6	11403.5415 ± 111.8892	35.7300 ± 0.1169	442.7992 ± 0.7209	16.7683 ± 0.0137
40.4	11370.6594 ± 111.3391	35.6956 ± 0.1165	440.2614 ± 0.7141	16.7164 ± 0.0135
60.0	11329.1724 ± 111.2379	35.6522 ± 0.1167	438.9205 ± 0.7127	16.6947 ± 0.0136
80.2	11281.8820 ± 110.7526	35.6025 ± 0.1165	437.6408 ± 0.7112	16.6704 ± 0.0135
100.2	11348.6381 ± 111.8371	35.6726 ± 0.1172	437.0391 ± 0.7077	16.6589 ± 0.0135

There are some important trends evident in this table. First, the total drag force and total cornering force increase in parallel. When a wing produces more lift, it also tends to produce more drag. The maximum drag force and maximum cornering force can thus be expected to occur at the same height, where the wing experiences maximum ground effect. This happens at a height of 19.6mm. Second, the maximum straight-line speed exhibits an inverse relationship with drag. When the drag is lower, the straight-line speed is lower. In contrast, the maximum cornering speed is higher for a higher cornering force. Once again, this highlights a tradeoff that has been measured and quantified experimentally

The lap times and uncertainty of the lap times can then easily be calculated as described in the methods section. The uncertainty is also computed. Both values are displayed on the table below. In addition, the lap time for a car without a wing is presented for comparison.

Table 4: Lap Time for Different Front Wing Heights

Wing height (mm)	Lap Time (s)
None	72.6530
1.2	70.7689 ± 0.0813
19.6	70.0991 ± 0.0829
40.4	70.2688 ± 0.0828
60.0	70.3583 ± 0.0831
80.2	70.4596 ± 0.0832
100.2	70.4485 ± 0.0833

The variations in the above table indicate a key pattern. First, the lap time without a wing is almost two seconds slower than all the others. In a sport such as F1 where margins are key, two seconds can mean the difference between first and tenth place. Second, the lap time at the lowest wing height is the slowest. This is due to the chaotic data, brought on by the flutter mode. The fastest lap time is at a height of 19.6mm, where the ground effect is strongest. The overall trends are plotted below and analyzed in more detail.

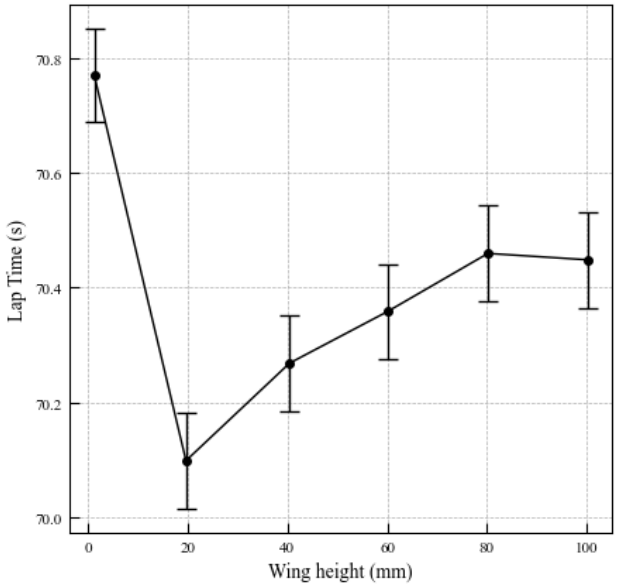

Figure 9: Overall Lap Time vs. Front Wing Height

This figure indicates the trend in lap time based on the experiment. At a low height, a porpoising (flutter) effect decreases the lap time. At a height of 20mm, where the wing is still in a strong ground effect, the car can corner well, and the lap time is fastest. As the wing height increases, the lift and drag values plateau. This effect is evident in the lap times, which appear to plateau as well.

IV. Uncertainty calculations

Given an arbitrary function of many variables, the overall uncertainty of the function is given by:

$$\sigma_f = \sqrt{\sum_{i=1}^{n} \left(\frac{\partial f}{\partial x_i}\sigma_{x_i}\right)^2} \tag{22}$$

To obtain the overall uncertainty of the lap time, multiple intermediate uncertainties will be determined.

First, the uncertainty of a coefficient is a function of the uncertainty of the measured force and the wind tunnel velocity. The uncertainties of these quantities are described in the Methods section. The uncertainty of the lift coefficient is therefore:

$$\sigma_{C_L} = \sqrt{\left(\frac{-2F_L}{\rho S V^3}\sigma_V\right)^2 + \left(\frac{2 \cdot 53.411}{\rho S V^2}\sigma_{L_{\text{volt}}}\right)^2}$$

And the uncertainty of the drag coefficient is obtained similarly as:

$$\sigma_{C_D} = \sqrt{\left(\frac{-2F_D}{\rho S V^3}\sigma_V\right)^2 + \left(\frac{2 \cdot 53.411}{\rho S V^2}\sigma_{D_{\text{volt}}}\right)^2}$$

In order to calculate the maximum straight line speed, the drag force is obtained. The uncertainty of the drag force in a straight line is:

$$\sigma_{F_D} = \frac{1}{2}\rho \frac{P\, A_{\text{wing}}}{\left(C_{D,\text{car}}A_{\text{car}} + C_{D,\text{wing}}A_{\text{wing}}\right)^2}\sigma_{C_{D,\text{wing}}}$$

This can be used to calculate the uncertainty of the maximum straight line speed:

$$\sigma_{V_s} = \frac{A_{\text{wing}}}{3}\left(\frac{2P}{\rho}\right)^{\frac{1}{3}}\left(C_{D,\text{car}}A_{\text{car}} + C_{D,\text{wing}}A_{\text{wing}}\right)^{-\frac{4}{3}}\sigma_{C_{D,\text{wing}}}$$

Similarly, the uncertainties of the maximum cornering speed must be calculated. The uncertainty of the cornering force is obtained as:

$$\sigma_{F_{\text{corner}}} = \frac{1}{2}a\,\rho\, V_c^2\, A_{\text{wing}}\sigma_{C_{L,\text{wing}}}$$

This can be used to solve the uncertainty of the maximum cornering velocity:

$$\sigma_{V_c} = \frac{a\rho\, A_{\text{wing}}}{4}\frac{\sqrt{a\, m\, g + b}}{\left(\frac{m}{r} + \frac{a}{2}\rho\left(C_{L,\text{car}}A_{\text{car}} + C_{L,\text{wing}}A_{\text{wing}}\right)\right)^{3/2}}\sigma_{C_{L,\text{wing}}}$$

Using the uncertainties for the velocities, the uncertainty of the lap time can be computed:

$$\sigma_{t_{\text{lap}}} = \sqrt{\left(\frac{800}{V_s^2}\sigma_{V_s}\right)^2 + \left(\frac{800}{V_c^2}\sigma_{V_c}\right)^2}$$

The uncertainty of the lap time can be converted to a percent relative uncertainty:

$$\sigma_{t_{lap},percent} = \frac{\sigma_{t_{lap}}}{t_{lap}}100\%$$

These uncertainty equations were implemented in Python. The code is available in the appendix.

V. Conclusion

In conclusion, this experiment successfully investigated the impact of front wing height on Formula 1 car performance through wind tunnel testing and subsequent lap time modeling. Based on the experimental results, wing height affects aerodynamic performance and as a result the overall lap times. The optimal height identified was at 19.6mm where the wing experiences maximum ground effect. At this height, the car achieved a predicted lap time of 70.0991 ± 0.0829 seconds, approximately 2.5 seconds faster than a car without a wing, highlighting the critical importance of well-tuned aerodynamics in competitive racing.

The experiment revealed several important aerodynamic phenomena. At extremely low heights (1.2mm), a flutter mode resembling the "porpoising" effect observed in real F1 cars created unstable aerodynamic conditions, resulting in chaotic data and reduced performance. As the wing height increased beyond the optimal position, both lift and drag coefficients gradually decreased and plateaued, indicating diminished ground effect influence. This relationship between wing height and aerodynamic coefficients directly translated to vehicle performance metrics, where maximum cornering speed and maximum straight-line speed showed clear trade-offs across different wing configurations.

The experimental data also confirmed the expected inverse relationship between drag force and maximum straight-line speed. In addition, the downforce and cornering capability are positively correlated. This quantifies the trade-off racing engineers face when optimizing aerodynamic setups: increasing downforce improves cornering performance but typically reduces straight-line speed due to increased drag. Our lap time model effectively captured this balance, showing that intermediate wing heights provide the best overall performance by optimizing the balance between these competing factors.

Despite the valuable insights gained, several experimental limitations affected the accuracy of our results. The wind tunnel's flow fluctuations introduced some measurement uncertainty, while the ground condition and confined flow affected the ground effect measurements. The lap time model, which assumes instantaneous acceleration and deceleration between corners and straights and linear relationships between downforce and cornering force, represents a significant simplification of real-world racing. In a true F1 race, braking, acceleration, and varying tire performance play important roles.

Future experiments should address these limitations by utilizing more sophisticated wind tunnels with better flow uniformity, implementing more realistic ground conditions, and developing a more comprehensive lap time model that incorporates transient vehicle dynamics. Directly comparing CFD with wind tunnel results would help to validate the experiment. Additionally, investigating the effects of wing angle, different wing geometries, and different car configurations would produce better lap times. These improvements would enhance understanding of aerodynamic optimization in competitive motorsport applications and lead to more precise performance predictions.

Appendix

A. Raw output of analysis code

The raw output of the analysis code is included below:

```
Uncertainty in C_L, C_D: 0.037407707542147034 0.05285003589567934
Height: 1.2 mm
  Max Velocity: 29.21 m/s
  C_L: 0.1783, C_D: 0.5373
  Total Drag Force: 11218.0531 ± 107.4508
  Straight-Line Velocity: 35.5352 ± 0.1135
  Cornering Force: 432.8158 ± 0.6820
  Cornering Velocity: 16.5782 ± 0.0131
  Lap Time: 70.7689 ± 0.0813

Uncertainty in C_L, C_D: 0.037777749352659706 0.053257323572592566
Height: 19.6 mm
  Max Velocity: 29.10 m/s
  C_L: 0.7135, C_D: 0.4476
  Total Drag Force: 11403.5415 ± 111.8892
  Straight-Line Velocity: 35.7300 ± 0.1169
  Cornering Force: 442.7992 ± 0.7209
  Cornering Velocity: 16.7683 ± 0.0137
  Lap Time: 70.0991 ± 0.0829

Uncertainty in C_L, C_D: 0.03777961615082986 0.05330243351088887
Height: 40.4 mm
  Max Velocity: 29.09 m/s
  C_L: 0.5692, C_D: 0.4633
  Total Drag Force: 11370.6594 ± 111.3391
  Straight-Line Velocity: 35.6956 ± 0.1165
  Cornering Force: 440.0614 ± 0.7121
  Cornering Velocity: 16.7164 ± 0.0135
  Lap Time: 70.2688 ± 0.0828

Uncertainty in C_L, C_D: 0.03801029674408602 0.05364472790032024
Height: 60.0 mm
  Max Velocity: 28.99 m/s
  C_L: 0.5085, C_D: 0.4832
  Total Drag Force: 11329.1724 ± 111.2379
  Straight-Line Velocity: 35.6522 ± 0.1167
  Cornering Force: 438.9205 ± 0.7127
  Cornering Velocity: 16.6947 ± 0.0136
  Lap Time: 70.3583 ± 0.0831

Uncertainty in C_L, C_D: 0.038150397884898796 0.05385943099466937
Height: 80.2 mm
  Max Velocity: 28.94 m/s
  C_L: 0.4400, C_D: 0.5061
  Total Drag Force: 11281.8820 ± 110.7526
  Straight-Line Velocity: 35.6025 ± 0.1165
  Cornering Force: 437.6408 ± 0.7112
  Cornering Velocity: 16.6704 ± 0.0135
  Lap Time: 70.4596 ± 0.0832

Uncertainty in C_L, C_D: 0.03807028971496331 0.053748856500569736
Height: 100.2 mm
  Max Velocity: 28.97 m/s
  C_L: 0.4077, C_D: 0.4738
  Total Drag Force: 11348.6381 ± 111.8371
  Straight-Line Velocity: 35.6726 ± 0.1172
  Cornering Force: 437.0391 ± 0.7077
  Cornering Velocity: 16.6589 ± 0.0135
  Lap Time: 70.4485 ± 0.0833
```

B. Python Uncertainty Calculations

The source code to compute the results and efficiency is included below.

```
import numpy as np
import matplotlib as mpl
import matplotlib.pyplot as plt

# --- Previously defined functions ---
def voltage_to_force(lift_voltage, drag_voltage):
    """Convert load cell voltages to forces in Newtons."""
    F_L = 53.411 * lift_voltage - 0.2353
    F_D = 75.424 * drag_voltage + 0.0971
    return F_L, F_D

def compute_coefficients(V, F_L, F_D, S, rho=1.0):
    """Compute lift and drag coefficients."""
    q = 0.5 * rho * V**2  # Dynamic pressure
    C_L = F_L / (q * S)
    C_D = F_D / (q * S)
    return C_L, C_D

def reynolds_number(V, L=0.1, nu=1.49e-5):
    return (V * L) / nu

def plot_coeff_vs_reynolds(data, S, lift=True):
    """Plot Lift Coefficient (C_L) or Drag Coefficient (C_D) as a function of Reynolds Number
(Re)."""
    plt.figure()
    for i, (H, dataset) in enumerate(data.items()):
        V, L_volt, D_volt = dataset.T
        F_L, F_D = voltage_to_force(L_volt, D_volt)
        C_L, C_D = compute_coefficients(V, F_L, F_D,S)
        Re = reynolds_number(V)
        color = grayscale_styles[i % len(grayscale_styles)]
        marker = markers[i % len(markers)]
        if lift:
            plt.plot(Re, C_L, color, marker=marker, label=f"H = {H:.1f} mm", markersize=5)
            plt.ylabel("Lift Coefficient, C_L")
            plt.title("Lift Coefficient vs. Reynolds Number")
        else:
            plt.plot(Re, C_D, color, marker=marker, label=f"H = {H:.1f} mm", markersize=5)
            plt.ylabel("Drag Coefficient, C_D")
            plt.title("Drag Coefficient vs. Reynolds Number")
    plt.xlabel("Reynolds Number, Re")
    plt.legend()
    plt.xscale("log")
    plt.tight_layout()
    plt.show()

def calculate_drag_and_velocity(C_D_wing, A_wing):
    """
    Calculate total drag force (F_D) and maximum straight-line velocity (V_s).
    """
    total_C_D = C_D_car * A_car + C_D_wing * A_wing
    # F_D = 0.5 * rho * P / (total_C_D)
    F_D = 0.5 * rho * P / total_C_D  # as given in the original formulation
    V_s = np.cbrt(2 * P / (rho * total_C_D))
    return F_D, V_s

def calculate_uncertainty_drag_velocity(C_D_wing, A_wing, sigma_CD_wing):
    """
    Calculate uncertainty in total drag force (F_D) and maximum straight-line velocity (V_s).
    """
    total_C_D = C_D_car * A_car + C_D_wing * A_wing
    # Using: sigma_{F_D} = (0.5*rho*P*A_wing/(total_C_D^2))*sigma_CD_wing
    sigma_F_D = 0.5 * rho * P * A_wing / (total_C_D**2) * sigma_CD_wing
    # Using: sigma_{V_s} = (A_wing/3)*(2P/rho)**(1/3)*(total_C_D)**(-4/3)*sigma_CD_wing
    sigma_V_s = (A_wing / 3) * (2 * P / rho)**(1/3) * (total_C_D)**(-4/3) * sigma_CD_wing
    return sigma_F_D, sigma_V_s

def calculate_cornering(a, m, g, b, C_L_car, C_L_wing, A_car, A_wing, r, rho):
```

```
    """
    Calculate the cornering force and cornering velocity using the updated equation:

      (m V_c^2)/r = a*(0.5*rho*V_c^2*(C_L_car*A_car + C_L_wing*A_wing) + m*g) + b

    Solving for V_c gives:

      V_c = sqrt((a*m*g + b) / ((m/r) - (a*rho*(C_L_car*A_car + C_L_wing*A_wing))/2))

    The cornering force is defined as:

      F_corner = m*V_c^2 / r.
    """
    C_sum = C_L_car * A_car + C_L_wing * A_wing
    denominator = (m / r) - (a * rho * C_sum) / 2
    numerator = a * m * g + b
    V_c = np.sqrt(numerator / denominator)
    F_corner = m * V_c**2 / r
    return F_corner, V_c

def  calculate_uncertainty_cornering(a,  m,  g,  b,  C_L_car,  C_L_wing,  A_car,  A_wing,  r,  rho,
sigma_C_L_wing):
    """
    Calculate the uncertainty in cornering force and cornering velocity using the updated equations,
    considering only the uncertainty in C_L_wing.

    The cornering velocity is given by:

      V_c = sqrt((a*m*g + b) / ((m/r) - (a*rho*(C_L_car*A_car + C_L_wing*A_wing))/2))

    and its derivative with respect to C_L_wing is:

              dV_c/d(C_L_wing)    =    (a*rho*A_wing/(4))    *    sqrt(a*m*g+b)    /    ((m/r    -
(a*rho*(C_L_car*A_car+C_L_wing*A_wing))/2)^(3/2)).

    Then, the uncertainty is:

      sigma_V_c = |dV_c/d(C_L_wing)| * sigma_C_L_wing,

    and for the cornering force:

      sigma_F_corner = (2*m*V_c/r)*sigma_V_c.
    """
    C_sum = C_L_car * A_car + C_L_wing * A_wing
    denominator = (m / r) - (a * rho * C_sum) / 2
    numerator = a * m * g + b
    V_c = np.sqrt(numerator / denominator)
    # Compute derivative dV_c/d(C_L_wing)
    dV_c_dCLwing = (a * rho * A_wing / 4) * np.sqrt(numerator) / (denominator**(3/2))
    sigma_V_c = abs(dV_c_dCLwing) * sigma_C_L_wing
    sigma_F_corner = (2 * m * V_c / r) * sigma_V_c
    return sigma_F_corner, sigma_V_c

def compute_uncertainty(V, L_volt, D_volt, S, sigma_Voltage, sigma_V):
    """Calculate the uncertainty in C_L and C_D."""
    F_L = 53.411 * L_volt - 0.2353
    F_D = 75.424 * D_volt + 0.0971
    C_L = (2 * F_L) / (rho * S * V**2)
    C_D = (2 * F_D) / (rho * S * V**2)
    dCL_dV = -2 * F_L / (rho * S * V**3)
    dCL_dLvolt = (2 * 53.411) / (rho * S * V**2)
    dCD_dV = -2 * F_D / (rho * S * V**3)
    dCD_dDvolt = (2 * 75.424) / (rho * S * V**2)
    sigma_CL = np.sqrt((dCL_dV * sigma_V)**2 + (dCL_dLvolt * sigma_Voltage)**2)
    sigma_CD = np.sqrt((dCD_dV * sigma_V)**2 + (dCD_dDvolt * sigma_Voltage)**2)
    return sigma_CL, sigma_CD

def calc_laptime(v_s, v_c, ss, sc):
    sigma = np.sqrt((800/v_s/v_s * ss)**2 + (800/v_c/v_c * sc)**2)
    return 800 * (1 / v_s + 1 / v_c), sigma
```

References

[1] NASCAR. "Complete List of NASCAR Regional Tracks." NASCAR.com, 25 Feb. 2025, https://www.nascar.com/news-media/2025/02/25/nascar-regional-tracks/.
[2] Donate Dsouza, Royson. "Diagram of a Closed Type Wind Tunnel." Wind Tunnels: State of Art Survey and Future Scope for Testing Micro Air Vehicles, ResearchGate, https://www.researchgate.net/figure/Diagram-of-a-Closed-Type-Wind-Tunnel_fig4_303806420.
[3] USU MAE Dept. “Formula One Lab Overview”, *MAE 4400 Canvas.* 2025

AI Disclosure

Artificial Intelligence was used to write analysis formulas & code and construct sections of the conclusion and abstract.